Wnt/β-catenin-YAP axis in the pathogenesis of primary intraosseous carcinoma NOS, deriving from odontogenic keratocyst

Nakako, Yusuke
Laboratory of Oral Pathology, Division of Maxillofacial Diagnostic and Surgical Sciences, Faculty of Dental Science, Kyushu University

Hasegawa, Kana
Laboratory of Oral Pathology, Division of Maxillofacial Diagnostic and Surgical Sciences, Faculty of Dental Science, Kyushu University

Fujii, Shinsuke
Laboratory of Oral Pathology, Division of Maxillofacial Diagnostic and Surgical Sciences, Faculty of Dental Science, Kyushu University

Kami, Yukiko
Department of Oral and Maxillofacial Radiology, Faculty of Dental Science, Kyushu University

他

出版情報：Pathology - Research and Practice. 260, pp.155420-, 2024-08. Elsevier
バージョン：

Pathology - Research and Practice 260 (2024) 155420

Contents lists available at ScienceDirect

Pathology - Research and Practice

journal homepage: www.elsevier.com/locate/prp

Wnt/β-catenin-YAP axis in the pathogenesis of primary intraosseous carcinoma NOS, deriving from odontogenic keratocyst

Yusuke Nakako [a,b,1], Kana Hasegawa [a,1], Shinsuke Fujii [a,c,d,*], Yukiko Kami [e], Taiki Sakamoto [b], Mizuki Sakamoto [b], Masafumi Moriyama [f], Kari J. Kurppa [d], Kristiina Heikinheimo [g], Kazunori Yoshiura [e], Shintaro Kawano [b], Tamotsu Kiyoshima [a]

[a] *Laboratory of Oral Pathology, Division of Maxillofacial Diagnostic and Surgical Sciences, Faculty of Dental Science, Kyushu University, 3-1-1 Maidashi, Higashi-ku, Fukuoka 812-8582, Japan*

[b] *Section of Oral and Maxillofacial Oncology, Division of Maxillofacial Diagnostic and Surgical Sciences, Faculty of Dental Science, Kyushu University, 3-1-1 Maidashi, Higashi-ku, Fukuoka 812-8582, Japan*

[c] *Dento-craniofacial Development and Regeneration Research Center, Faculty of Dental Science, Kyushu University, 3-1-1 Maidashi, Higashi-ku, Fukuoka 812-8582, Japan*

[d] *Institute of Biomedicine and MediCity Research Laboratories, University of Turku, and Turku Bioscience Centre, University of Turku and Åbo Akademi University, Turku 20520, Finland*

[e] *Department of Oral and Maxillofacial Radiology, Faculty of Dental Science, Kyushu University, Fukuoka, Japan*

[f] *Section of Oral and Maxillofacial Surgery, Division of Maxillofacial Diagnostic and Surgical Sciences, Faculty of Dental Science, Kyushu University, 3-1-1 Maidashi, Higashi-ku, Fukuoka 812-8582, Japan*

[g] *Department of Oral and Maxillofacial Surgery, Institute of Dentistry, University of Turku and Turku University Hospital, 20520, Finland*

ARTICLE INFO

Key words:
Primary intraosseous carcinoma NOS (PIOC)
Mandible
Wnt/β-catenin
YAP
Odontogenic keratocyst

ABSTRACT

Odontogenic tumors (OGTs), which originate from cells of odontogenic apparatus and their remnants, are rare entities. Primary intraosseous carcinoma NOS (PIOC), is one of the OGTs, but it is even rarer and has a worse prognosis. The precise characteristics of PIOC, especially in immunohistochemical features and its pathogenesis, remain unclear. We characterized a case of PIOC arising from the left mandible, in which histopathological findings showed a transition from the odontogenic keratocyst to the carcinoma. Remarkably, the tumor lesion of this PIOC prominently exhibits malignant attributes, including invasive growth of carcinoma cell infiltration into the bone tissue, an elevated Ki-67 index, and lower signal for CK13 and higher signal for CK17 compared with the non-tumor region, histopathologically and immunohistopathologically. Further immunohistochemical analyses demonstrated increased expression of ADP-ribosylation factor (ARF)-like 4c (ARL4C) (accompanying expression of β-catenin in the nucleus) and yes-associated protein (YAP) in the tumor lesion. On the other hand, YAP was expressed and the expression of ARL4C was hardly detected in the non-tumor region. In addition, quantitative RT-PCR analysis using RNAs and dot blot analysis using genomic DNA showed the activation of Wnt/β-catenin signaling and epigenetic alterations, such as an increase of 5mC levels and a decrease of 5hmC levels, in the tumor lesion. A DNA microarray and a gene set enrichment analysis demonstrated that various types of intracellular signaling would be activated and several kinds of cellular functions would be altered in the pathogenesis of PIOC. Experiments with the GSK-3 inhibitor revealed that β-catenin pathway increased not only mRNA levels of *ankyrin repeat domain1* (*ANKRD1*) but also protein levels of YAP and transcriptional co-activator with PDZ-binding motif (TAZ) in oral squamous cell carcinoma cell lines. These results suggested that further activation of YAP signaling by Wnt/β-catenin signaling may be associated with the pathogenesis of PIOC deriving from odontogenic keratocyst in which YAP signaling is activated.

* Corresponding author at: Laboratory of Oral Pathology, Division of Maxillofacial Diagnostic and Surgical Sciences, Faculty of Dental Science, Kyushu University, 3-1-l Maidashi, Higashi-ku, Fukuoka 812-8582, Japan.
E-mail address: sfujii@dent.kyushu-u.ac.jp (S. Fujii).

[1] These authors contributed equally to this work.

https://doi.org/10.1016/j.prp.2024.155420
Received 18 March 2024; Received in revised form 14 June 2024; Accepted 19 June 2024
Available online 20 June 2024

1. Introduction

Odontogenic tumors (OGTs), which originate from cells of odontogenic apparatus and their remnants, are rare, constituting < 1 % of all oral tumors [1]. Most OGTs are benign, and malignant OGTs are low incidence rate with 0.3–5.7 % of all OGTs [2]. Both benign and malignant OGTs are subclassified into epithelial tumors, mixed epithelial and mesenchymal tumors and mesenchymal tumors. In addition, malignant OGTs are classified into odontogenic carcinoma, odontogenic carcinosarcoma and odontogenic sarcoma. Odontogenic carcinoma consists of ameloblastic carcinoma, primary intraosseous carcinoma NOS (PIOC), sclerosing odontogenic carcinoma, clear cell odontogenic carcinoma and ghost cell odontogenic carcinoma [1].

PIOC, which frequently occurs in the posterior body and ramus of the mandible, cannot be categorized as any other type of carcinoma. Carcinoma arising in the oral mucosa and infiltrating the mandible, an antral primary and metastatic carcinoma must be excluded, and ulceration to the oral cavity is normally considered to preclude definitive diagnosis [1]. PIOC is a rare entity and cases arising in cysts are more common in the mandible [3,4]. In PIOC occurrence, radicular/residual cysts are the most common precursors, followed by dentigerous cysts and odontogenic keratocysts [1]. Radiographically, cases arising in cysts may produce an apparently multilocular or scalloped radiolucency. When the tumor is detected early, the radiological features appear benign one and the carcinoma is an incidental histological finding on enucleation [5,6]. When cases arise in odontogenic cysts, there may be a histological transition between the benign precursor and the carcinoma. Although an insufficient number of cases has been reported to determine outcome, prognosis is generally poor [1]. Several reports have demonstrated that the 5-year survival rate of reported case with PIOC is 52 % [5,6]. Therefore, new anticancer therapies based on the molecular mechanisms underlying PIOC tumorigenesis are needed.

We recently reported several activated intracellular signaling molecules, such as ADP-ribosylation factor (ARF)-like 4c (ARL4C) [7–9] and yes-associated protein (YAP) [10,11], may be not only specific markers of oral epithelial tumors but also exerting an oncogenic role in their tumorigenesis. However, the characteristics of PIOC, including its immunohistochemical features, such as ARL4C and YAP expression, are unclear.

In the present report, we conducted a study using a rare case of PIOC pathological specimen, which appeared to be derived from odontogenic keratocyst, and cell lines to elucidate the role of Wnt/β-catenin-YAP axis in the pathogenesis of PIOC.

2. Material and methods

2.1. Patients and immunohistochemistry

A 79-year-old female, the case of this person is mentioned below, and total of 5 patients with odontogenic keratocyst diagnosed for treatment at the Department of Oral and Maxillofacial Surgery, Kyushu University Hospital, Japan from May 2021 to May 2023 were examined. Details for each patient were as follows; #1, 65-year-old, male, mandible; #2, 21-year-old, female, mandible; #3, 40-year-old, female, mandible; #4, 26-year-old, female, maxilla; #5, 75-year-old, female, mandible. The protocol for this study was approved by the ethical review board of the Local Ethical Committee of Kyushu University, Japan (#22433).

All specimens for histological examination were fixed in 10 % (v/v) neutral buffered formalin solution and embedded in paraffin blocks. The paraffin-embedded specimens were sliced into 4-μm-thick sections, stained with HE, and examined by three experienced pathologists to confirm the diagnoses. Immunohistochemical staining was performed on 4-μm-thick paraffin-embedded sections. Antigen retrieval, elimination of the endogenous peroxide activity, and blocking were carried out as previously described [11]. The sections were then incubated with each primary antibody (used at 1:300 for Ki-67, used at 1:100 for YAP, used at 1:100 for ARL4C, used at 1:2000 for CK13, used at 1:100 for CK17, used at 1:400 for β-catenin) at 4 ℃ overnight. The details of the antibodies used are mentioned below. The sections were incubated with secondary antibody (Histofine Simple Stain MAX PO, Nichirei, Tokyo, Japan) for 1 h at room temperature (RT). The immunoreactivity was visualized with a DAB substrate solution (Nichirei). Subsequently, the sections were counterstained with hematoxylin.

2.2. Cell lines and reagents

Human oral squamous cell carcinoma (OSCC) cell lines HSC-2 and HSC-3 (Japanese Cancer Research Resources Bank) were used in this study. HSC-2 and HSC-3 cells were maintained in α-MEM (Invitrogen, Carlsbad, CA, USA) with 10 % fetal bovine serum (Invitrogen) and contained 100 IU/ml penicillin and 100 mg/ml streptomycin (Invitrogen). All of these cell lines were incubated at 37 ℃ in a 5 % CO_2 atmosphere. When necessary, CHIR99021 (FUJIFILM Wako, Osaka, Japan) was added [12].

Anti-Ki-67 (M7240) (for immunohistochemistry), anti-β-catenin (M3539) (for immunohistochemistry) and anti-CK17 (M7046) (for immunohistochemistry) antibodies were obtained from Dako (Carpentaria, CA, USA). Anti-CK13 (ab16112) (for immunohistochemistry) and anti-double strand (ds) DNA (ab27156) (for dot blot) antibodies were purchased from Abcam (Cambridge, UK). Anti ARL4C (HPA028927) (for immunohistochemistry) antibody was obtained from Atlas Antibodies (Voltavägen, SWE). Anti-YAP (sc-101199) (for immunohistochemistry) antibody was purchased from Santa Cruz Biotechnology (Dallas, TX, USA). Anti-5mC (39649) (for dot blot) and anti-5hmC (39769) (for dot blot) antibodies were obtained from Active Motif (Carlsbad, CA, USA). Anti-β-catenin (610154) (for western blotting) antibody was purchased from BD biosciences (San José, CA, USA). Anti-YAP/TAZ (D24E4) (for western blotting) antibody was obtained from Cell signaling technology (Beverly, MA, USA). Anti-β-actin (A5441) (for western blotting) antibody was from Sigma-Aldrich (St. Louis, MO, USA).

2.3. RNA extraction, DNA extraction and quantitative RT-PCR

The total RNAs were isolated using the SV Total RNA Isolation System (Promega, Madison, WI, USA), and cDNAs were generated from isolated total RNAs using synthesized using ReverTra Ace qPCR RT Master Mix (TOYOBO, Osaka, Japan) according to the manufacturer's instructions. Then, the cDNA was used for quantitative PCR analysis [13]. Forward and reverse primers were as follows: human CK13, 5'-CCAACACTGCCATGATTCAG-3' and 5'-TCTGGCACTCCATCTCACTG-3'; human CK17, 5'-GCTGCTACAGCTTTGGCTCT-3' and 5'-TCACCTCCAGCTCAGTGT-3'; human Axin2, 5'-CTGGCTCCAGAAGATCACAAAG-3' and 5'-CATCCTCCCAGATCTCCTCAAA-3'; human Wnt1, 5'-CGGCGTTTATCTTCGCTATC-3' and 5'-GCCTCGTTGTTGTGAAGGTT-3'; human Wnt2b, 5'-AAGATGGTGCCAACTTCACC-3' and 5'-GCCACAGCACATGATTTCAC-3'; human Wnt3, 5'-ACTTTTGTGAGCCCAACCCA-3' and 5'-TTCTCCGTCCTCGTGTTGTG-3'; human Wnt4, 5'-GCTGTGACAGGACAGTGCAT-3' and 5'-GCCTCATTGTTGTGGAGGTT-3'; human Wnt7a, 5'-CCCACCTTCCTGAAGATCAA-3' and 5'-ACAGCACATGAGGTCACAGC-3'; human Wnt8a, 5'-CCATTGTCTATCCCCATTC-3' and 5'-GTGGGTGGAGAGCTGAAGAG-3'; human Wnt8b, 5'-TCGGAGAGGCGATTTCCAAG-3' and 5'-GTTGTGCAGGTTCATGGCTG-3'; human Wnt10a, 5'-AAGCTGCACCGCTTACAACT-3' and 5'-ATTCTCGCGTGGATGTCTCT-3'; human Wnt10b, 5'-GAAAACCTGAAGCGGAAATG-3' and 5'-GGGTCTCGCTCACAGAAGTC-3'; human Wnt16, 5'-GCTCCTGTGCTGTGAAAACA-3' and 5'-TGCATTCTCTG CCTTGTGTC-3'; human ARL4C, 5'-CTAACATCTCGGCCTTCCAG-3' and 5'-TCTGCTTGAGGGACTTCCTG-3'; human ANKRD1, 5'-ACGCCAAAGACAGAGAAGGA-3' and 5'-TTCTGCCAGTGTAGCACCAG-3'; human SNAI2, 5'-CTTTTTCTTGCCCTCACTGC-3' and 5'-ACAGCAGCCAGATTCCTCAT-3'; human DLX1, 5'-CAAGGCGGTGTTTATGGAGT-3' and 5'-TGCTGACCGAGTTGACGTAG-3'; human DLX2,

5'-GCACATGGGTTCCTACCAGT-3' and 5'-TCCTTCTCAGGCTCGT TGTT-3'; human IFT74, 5'-GGAAATAGCCAGCATGGAAA-3' and 5'-GTGCTCCAAGAGTGCAACAA-3'; human SIX1, 5'-CTCCTCCTCCAA-CAAGCAGA-3' and 5'-CTGTTAAGCCCGGGAGAGAA-3'; human GAPDH, 5'-GCACCGTCAAGGCTGAGAAC-3' and 5'-TGGTGAAGACG CCAGTGGA-3'.

2.4. Plasmid construction and infection using lentivirus harboring a cDNA

The YAP^{5SA} plasmid, CSII-CMV-MCS-IRES2-Bsd/FLAG-YAP^{5SA}, was used [10,14]. The vectors were transfected along with the packaging vectors, pCAG-HIV-gp (RDB04394) and pCMV-VSV-G-RSV-Rev (RDB04393), into X293T cells using the Lipofectamine LTX reagent (Invitrogen) to generate lentiviruses [15]. To generate OSCC cells that stably express YAP^{5SA} parental cells (5×10^4 cells/well in a 12-well plate) were treated with lentivirus and 10 μg/ml polybrene. The cells were then centrifuged at 1080 × g for 1 h, and incubated for another 24 h. The cells that demonstrated stable expression of YAP^{5SA} were selected and maintained in culture medium containing 5 μg/ml Blasticidin S (FUJIFILM Wako).

2.5. Dot blot analysis

Dot blot analysis was performed as previously described [7,11] with modification. Genomic DNA was diluted to 50 ng/μl in 20 μl total volume. 2.5 μl of 1 M NaOH was added to each sample and then the samples were incubated at 95 ℃ for 5 min. The samples were put on ice and neutralized with 3.3 μl of 5 M ammonium acetate. 2.1 μl and 1.05 μl of each mixture were spotted onto a nitrocellulose membrane and allowed to air dry for 10 min. The membrane was baked for 2 h at 80 ℃ and then blocked with 5 % milk for 2 h at RT. Anti-5hmC antibody (1:10000), anti-5mC antibody (1:1000) or anti-ds DNA antibody (1:1000) was incubated at 4 ℃ overnight, and subsequent incubation with goat anti-rabbit IgG-HRP or goat anti-mouse IgG-HRP for 2 h. ECL Western Blotting Detection Reagents (GE Healthcare, Chicago IL, USA) were used for detection.

2.6. DNA microarray analysis and gene set enrichment analyses

DNA microarray analysis was performed using RNAs extracted from the tumor lesion and the non-tumor region of PIOC. The gene set enrichment analyses (GSEA) analysis was performed as previously described [16]. The raw data reported in this study were deposited in NCBI GEO under the accession number (GSE24459003).

2.7. Immunofluorescence staining

HSC-3 and HSC-2 cells were fixed in 4 % (w/v) paraformaldehyde buffered by phosphate buffered saline (PBS) for 30 min at RT. After that, cells were permeabilized in PBS containing 0.5 % (w/v) Triton X-100 and 40 mg/ml BSA (FUJIFILM Wako) for 10 min at RT, and then blocked with 1 % BSA to prevent non-specific binding for 30 min at RT. The cells were incubated with primary antibody (used at 1:300 for β-catenin) for 3 h at RT, and then with secondary antibody (Jackson) and Hoechst 33342 (Dojindo, Kumamoto, Japan) for 2 h at RT. The samples were viewed with an All-in-one Fluorescence Microscope BZ 9000 (Keyence, Osaka, Japan) [17,18].

2.8. Immunoprecipitation

Immunoprecipitation was performed as described previously with modification [19]. HSC-3 cells expressing YAP^{5SA} (10 cm diameter dish) were lysed in 400 μl of NP40 buffer (20 mM Tris-HCl pH 8.0, 10 % glycerol, 137 mM NaCl and 1 % NP40) with protease inhibitors (2 % Protease inhibitor cocktail (Sigma-Aldrich), 1 μM Clasto-Lactacystin β-Lactone (Sigma-Aldrich), 25 mM β-glycerophosphate (Sigma-Aldrich), 1 mM Na_3VO_4 (Sigma-Aldrich) and 1 mM phenylmethanesulfonyl fluoride (FUJIFILM Wako)) for 10 min on ice. After centrifugation, the supernatant was collected and incubated with antibody for 1 h at 4 °C and further incubated with 40 μl of 50 % slurry of protein G Sepharose beads (GE healthcare) for 1 h at 4 °C. Beads were washed three times with 1 ml of NP40 buffer and were dissolved in Laemmli's sample buffer.

2.9. Statistical analysis

Statistical analyses were performed using JMP Pro 16 software. Significant differences were determined using one-way ANOVA with post hoc Tukey's test. P value of < 0.01 was considered to indicate statistical significance.

2.10. Additional assays

Western blotting was performed as described previously [20] and data were representative of at least three independent experiments.

3. Results

3.1. Clinical features and histological findings

A 79-year-old female visited at the Department of Oral and Maxillofacial Surgery at Kyushu University Hospital (Fukuoka, Japan) with exophytic swelling and pain in the left mandible, and fistula on the skin (Fig. 1A; left panel). She had no clinical evidence of cervical lymphadenopathy and no medical history of any significant diseases. An oral examination revealed the bulge of the left mandibular molar area without ulceration. A panoramic radiograph showed multilocular radiolucency (Fig. S1A). Computed tomography (CT) revealed a well-defined multilocular cystic lesion with high-density areas. Their density was approximately 100 Hounsfield Unit (HU), indicating a keratin-like material (Fig. 1A; right panel). Based on these findings, the lesion was clinically diagnosed as a benign lesion, such as odontogenic keratocyst or ameloblastoma, with no apparent findings with malignant tumors.

A biopsy was performed under local anesthesia. HE-stained sections showed cyst wall-structures lined by stratified squamous epithelium. Palisading of basaloid cells was seen in the lining epithelium and many keratin materials were observed in the cavity (Fig. 1B; left panels), which are histological findings similar to odontogenic keratocysts. In addition, the lesion included hyperparakeratinized lining epithelia, such as atypical verrucous hyperplasia with advanced stage, and budding-like elongation of rete ridges with atypical epithelial cells into subepithelial layer (Fig. 1B; right panels). Therefore, the lesion was histopathologically diagnosed as squamous cell carcinoma. Immunohistochemically, non-tumor region showed moderate Ki-67 index (24.2 % at the hot spot) (Fig. 1C; upper left panel). In contrast, the Ki-67 index was significantly elevated (69.3 % at the hot spot, $P<0.0001$) in the tumor lesion (Fig. 1C; upper right panel).

Immunohistochemical analyses showed that the cyst lining epithelial cells were positive for CK13 and weakly positive for CK17 in the non-tumor region (Fig. S1B; upper and middle left panels). Pathological meanings of this weak positive for CK17 in the non-tumor region remained unclear. In contrast, decreased signal for CK13 and increased signal for CK17 were noted in the tumor lesion (Fig. S1B; upper and middle right panels). As OSCC is characterized by an increase in CK17 and a decrease in CK13 [21–23], it is suggested that the lesion exhibits malignant potential, immunohistochmically. β-catenin was detected in the cell membrane of squamous cells both in the non-tumor region and in the tumor lesion (Fig. S1B; lower panels). Based on these histological and immunohistochemical findings, the lesion was suspected as PIOC, potentially derived from odontogenic keratocyst.

To profile the tumor lesion, further immunohistochemical analyses

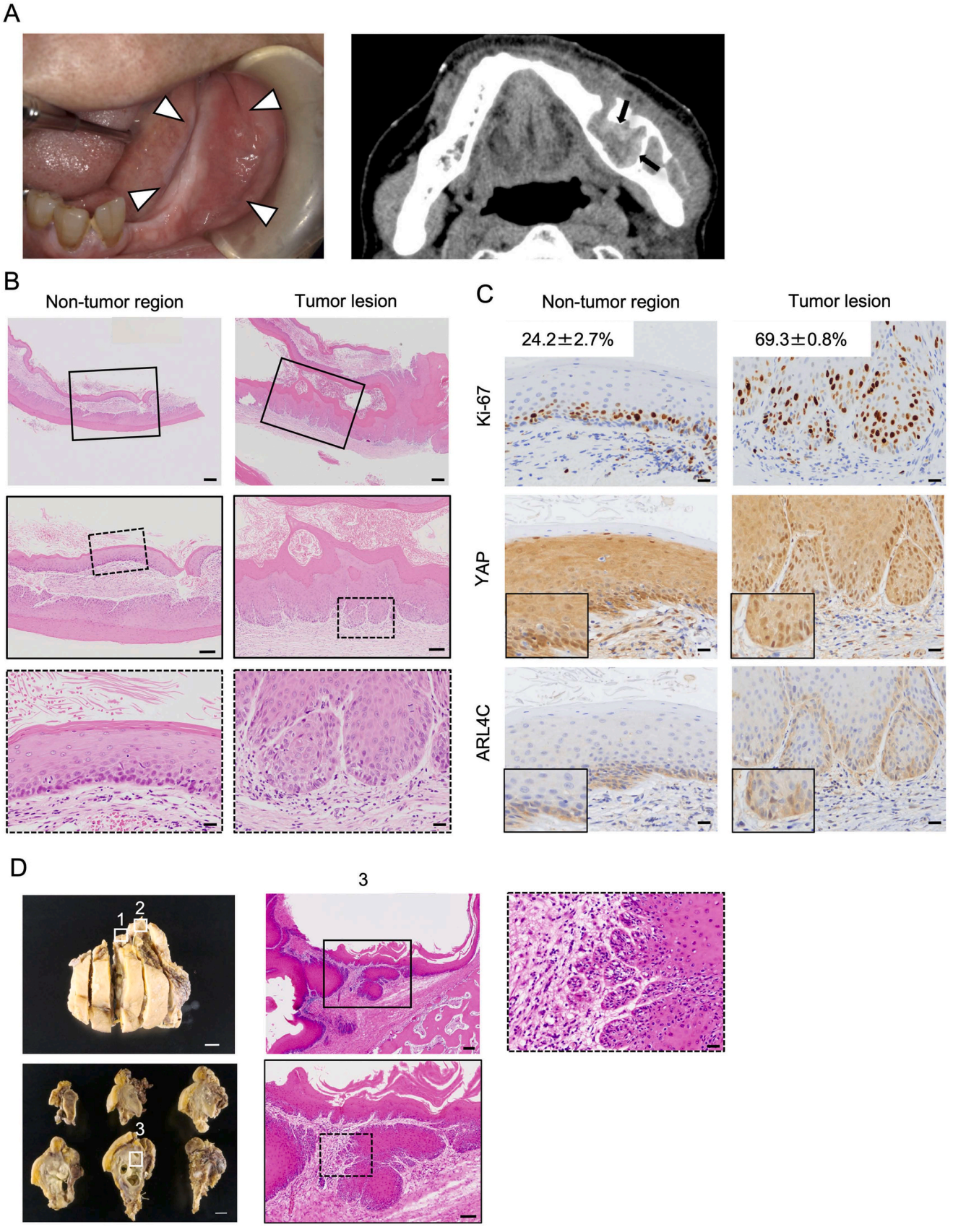

(caption on next page)

Fig. 1. Clinical features and histological findings of the primary intraosseous carcinoma NOS. (A) A mass (white arrowheads) in the left mandible was shown in a clinical photograph (left panel). Image of CT (right panel). Black arrows indicate keratin-like material in the cystic lesion of the left mandible. (B) HE staining of the biopsy of the left mandibular molar area with non-tumor region and tumor lesion. The solid box and the dashed box indicate enlarged images. Non-tumor region and tumor lesion in the Fig. 1B and 1C are consecutive sections. (C) The sections of (B) were stained with anti-Ki-67, YAP and ARL4C antibodies and hematoxylin. Ki-67 index was shown in the upper left. (D) A macroscopic photograph of the surgical resection sample, which were 87 × 59 × 73 mm (left panels). HE staining of the surgical resection sample of area 3 (right panels). The samples of area 1 and area 2 were used in Fig 2A. The solid box and the dashed box indicate enlarged images. Scale bars, 10 mm (D; left panels), 200 μm (B; upper panels and D; upper middle panel), 100 μm (B; middle panels and D; lower middle panel), 20 μm (B; lower panels, C, and D; right panel).

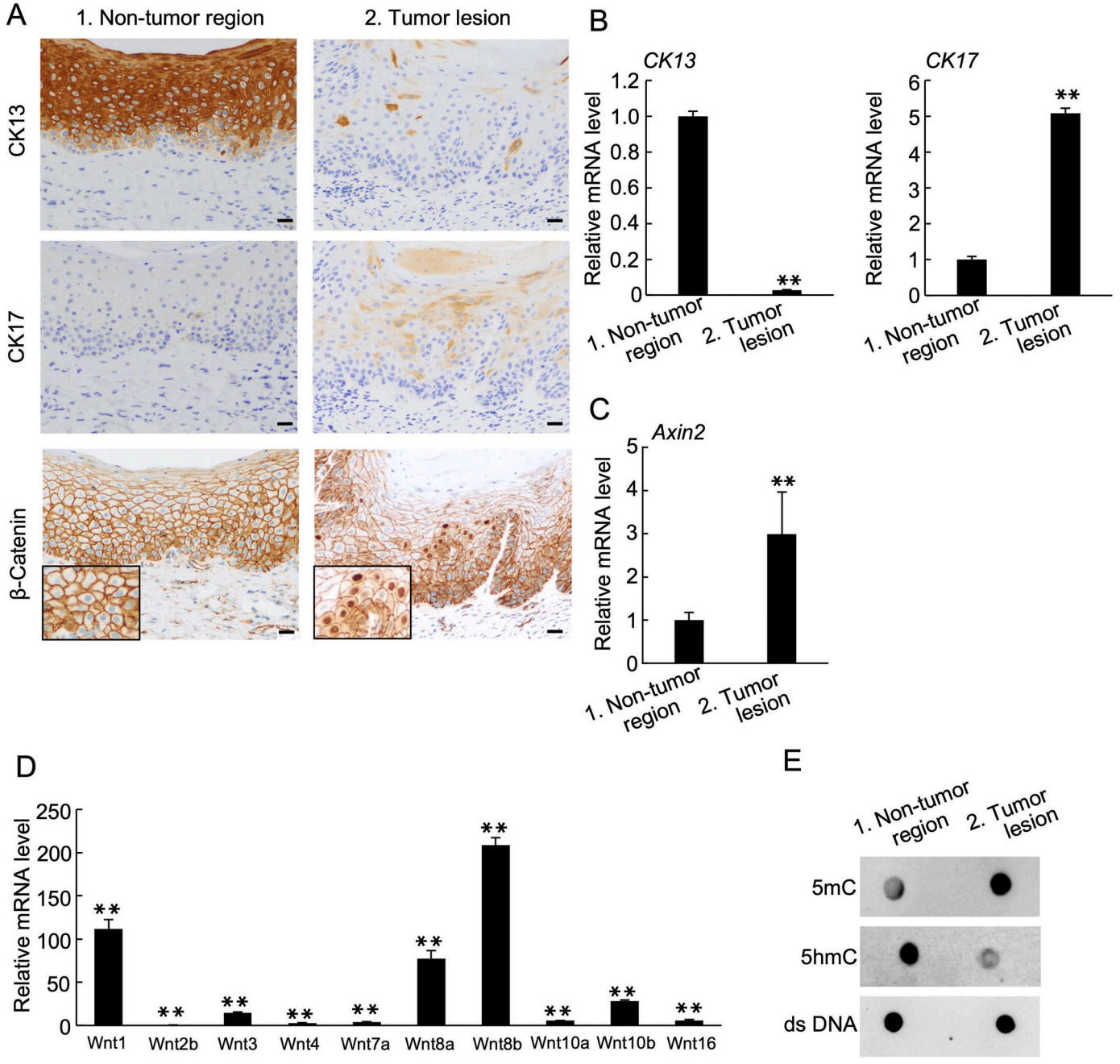

Fig. 2. Characterization of the primary intraosseous carcinoma NOS. (A) The surgically resected specimens with non-tumor region and tumor lesion (indicated in Fig. 1D) were stained with anti-CK13, CK17 and β-catenin antibodies as well as hematoxylin. (B) *CK13* and *CK17* mRNA levels were measured in non-tumor region and tumor lesion of PIOC. *CK13* and *CK17* mRNA levels were normalized by *GAPDH* and expressed as fold-changes compared with levels in non-tumor region. (C) *Axin2* mRNA levels were measured in non-tumor region and tumor lesion of PIOC. *Axin2* mRNA levels were normalized by *GAPDH* and expressed as fold-changes compared with levels in non-tumor region. (D) *Wnt1*, *Wnt2b*, *Wnt3*, *Wnt4*, *Wnt7a*, *Wnt8a*, *Wnt8b*, *Wnt10a*, *Wnt10b* and *Wnt16* mRNA levels were measured in non-tumor region and tumor lesion. These mRNA levels were normalized by *GAPDH* and these levels in tumor lesion were expressed as fold-changes compared with levels in non-tumor region of PIOC. (E) Analysis of 5mC and 5hmC levels in genomic DNA isolated from non-tumor region and tumor lesion of PIOC was performed by dot blot assay using an anti-5mC and anti-5hmC antibodies. Anti-ds DNA antibody was probed as a control. Scale bars, 20 μm. Results are shown as means ± s.d. of three independent experiments. $^{**}P<0.01$.

were performed. The Hippo pathway regulates cell proliferation through the nuclear localization of major downstream effectors, YAP and transcriptional co-activator with PDZ-binding motif (TAZ), resulting in the induction of target gene transcription [24,25]. We have recently demonstrated that YAP signaling regulates OSCC cell proliferation [10]. Indeed, YAP was detected in the nucleus of the atypical epithelial cells in the tumor lesion, suggesting YAP activation in these cells (Fig. 1C; middle right panel). Surprisingly, YAP was also detected in the nucleus of the parabasal and/or basal layer in the non-tumor region (Fig. 1C; middle left panel). Previous report demonstrated that YAP was especially detected in the nucleus of basaloid cells in the pathological specimens of odontogenic keratocyst [26], which was confirmed by our immunohistochemical analyses (Fig. S2; second panels from the left). β-catenin was detected in the cell membrane of squamous cells in the region (Fig. S2; rightmost panels). These data suggested that the immunohistochemical characteristics of epithelial cells in the non-tumor region might be similar to those of odontogenic keratocyst (Fig. 1C; middle left panel).

The expression of ARL4C is upregulated in several tumors and associated with tumorigenesis [8,14], and promotes proliferation in OSCC cells [9]. Consistent with these reports, the expression of ARL4C was highly detected in cytoplasm at the invasion front of the tumor lesion but its expression was only seen in the basal cells of the non-tumor region (Fig. 1 C; lower panels). The expression of ARL4C in the present non-tumor region appeared to be higher than those of the specimens with odontogenic keratocyst (Fig. S2; second panels from the right), suggesting that the characteristics of the present non-tumor region might be different from those of odontogenic keratocyst. However, its pathological meanings remained unclear. Based on these immunohistochemical analyses, the tumor lesion may exhibit malignant potential. Therefore, after 1 month later of the biopsy, a surgical resection was carried out and HE-stained section, of which section was indicated as area 3 in the picture, showed an invasive growth of carcinoma cells into the bone tissue (Fig. 1D). Based on the results from the histological and immunohistochemical analyses, the lesion was diagnosed as PIOC. In addition, we observed that both YAP and ARL4C signaling were activated in the tumor.

3.2. Characterization of the PIOC

From the surgical resection sample, we collected tissues from non-tumor region, (area 1, Fig. 1D; left panels), and from tumor lesion, (area 2, Fig. 1D; left panels). The tissue samples were clinically diagnosed and collected by an oral surgeon. We divided each sample into two specimens with or without formalin fixation.

Immunohistochemical analyses showed that the cyst lining epithelial cells were positive for CK13 and negative for CK17 in the non-tumor region (Fig. 2A; upper and middle left panels). In contrast, decreased signal for CK13 and increased signal for CK17 were noted in the tumor lesion (Fig. 2 A; upper and middle right panels). To assess the expression of *CK13* and *CK17*, RNA was extracted from the non-fixed specimens. Consistent with the immunohistochemical findings, *CK13* mRNA expression was decreased and *CK17* mRNA expression was increased in the tumor lesion and vice versa in the non-tumor region (Fig. 2B). YAP was detected both in the nucleus of the atypical epithelial cells in the tumor lesion and the parabasal and/or basal layer in the non-tumor region (Fig. S3; upper panels). The expression of ARL4C was detected in cytoplasm at the invasion front of the tumor lesion but its expression was only seen in the basal cells of the non-tumor region (Fig. S3; lower panels). Consistent with the findings of the biopsy, these analyses demonstrate that the PIOC tumor lesion shows features of OSCC.

Wnt/β-catenin signaling has been reported to be involved in the disease pathogenesis as well as in the developmental processes [27,28]. As no mutations in components of Wnt/β-catenin signaling have been identified in OSCC pathological specimens or cell lines [29–31], the activation of Wnt/β-catenin signaling would be unlikely to be involved in OSCC tumorigenesis. Here, β-catenin was sparsely detected in the nucleus of the tumor lesion (Fig. 2A; lower right panel) and the expression of *Axin2* (a direct target gene of the Wnt/β-catenin signaling [32]) was increased in the lesion (Fig. 2C), suggesting focal activation of the Wnt/β-catenin signaling in PIOC. Wnt ligand consists of 19 members [28]. Among them, the expression of Wnt ligands, which activates Wnt/β-catenin-dependent signaling [33], such as *Wnt1*, *Wnt2b*, *Wnt3*, *Wnt4*, *Wnt7a*, *Wnt8a*, *Wnt8b*, *Wnt10b* and *Wnt16*, was higher in the tumor lesion than in the non-tumor region (Fig. 2D). Based on these results, PIOC was characterized by focal activation of Wnt/β-catenin signaling potentially due to increased expression of some Wnt ligands.

Furthermore, as changes in DNA methylation are associated with tumorigenesis [34], the global DNA methylation status in the tumor lesion was analyzed. 5-methylcytosine (5mC), a global DNA methylation marker, was increased in the tumor lesion, while 5-hydroxymethylcytosine (5hmC), which is converted from 5mC to promote transcriptional activity [35], was reduced (Fig. 2E). These results suggested that PIOC is associated with epigenetic changes which may affect gene expression in the tumor cells.

To further clarify the characteristics of the present PIOC, a DNA microarray analysis was performed from the RNA, which were used in quantitative RT-PCR analyses (Fig. 2B and 2C). Fig. 3A shows scatterplots representing differences in gene expression amounts comparing the tumor lesion and the non-tumor region. As we recently identified the target molecules and signaling using the DNA microarray analysis based on the criteria of which expression is 1.5 fold change [12,13], we followed these criteria in this study. The expression of 389 genes was upregulated and the expression of 581 genes was downregulated in the tumor lesions. Especially, the expression of *CK17* was higher and the expression of *CK13* was lower in the tumor lesion (Fig. 3A). These expression patterns were consistent with previous our report [9] and the data with immunohistochemical findings and quantitative RT-PCR analysis (Fig. 2A and 2B), suggesting that the current DNA microarray data would reflect genetic background in the present PIOC. We further conducted GSEA analysis. The gene sets “WNT BETA CATENIN SIGNALING”, “NOTCH SIGNALING”, “KRAS SIGNALING”, “P53 PATHWAY”, “MTORC1 SIGNALING”, “TGF BETA SIGNALING”, “COMPLEMENT”, “INFLAMMATORY RESPONSE”, “HYPOXIA” and “APOPTOSIS” were significantly upregulated in the tumor lesion (Fig. 3B). Among them, Notch signaling pathway was ranked as an activated gene set in the tumor lesion (Fig. 3B). Notch signaling pathway is involved in tumorigenesis including OSCC [36,37]. The expression of Notch signaling pathway target genes, such as *SNAI2*, *DLX1*, *DLX2*, *IFT74* and *SIX1*, was indeed upregulated in the tumor lesion by quantitative RT-PCR analysis (Fig. S4). These data suggested that various types of intracellular signaling would be activated and several kinds of cellular functions would be altered in the pathogenesis of PIOC.

3.3. Wnt/β-catenin signaling activates YAP signaling in OSCC cells

In this PIOC, squamous cell carcinoma cells were invaded into the subepithelial layer and the bone tissue (see Fig. 1B; right panels and Fig. 1D). We have recently demonstrated that YAP signaling is activated in OSCC cells [10]. It has been reported that Wnt/β-catenin signaling regulates YAP activity at the protein or transcriptional level [38,39]. Since the effect of Wnt/β-catenin signaling on YAP signaling remains unclear in OSCC, we used OSCC cell lines to investigate its effect. Human OSCC cells, HSC-2 and HSC-3 cells were treated with the GSK-3 inhibitor, CHIR99021, which is an activator of the β-catenin pathway [19,40]. The protein levels and nuclear translocation of β-catenin were increased by CHIR99021 treatment (Fig. 4A and Fig. S5A). Consistent with previous reports [8,14], treatment with CHIR99021 induced the expression of *ARL4C* (Fig. 4B; left graph and Fig. S5B; left graph). In addition, the treatment increased the mRNA levels of *ankyrin repeat domain1* (*ANKRD1*, a direct target gene of the YAP signaling) (Fig. 4B; right graph and Fig. S5B; right graph), and the protein levels of YAP and

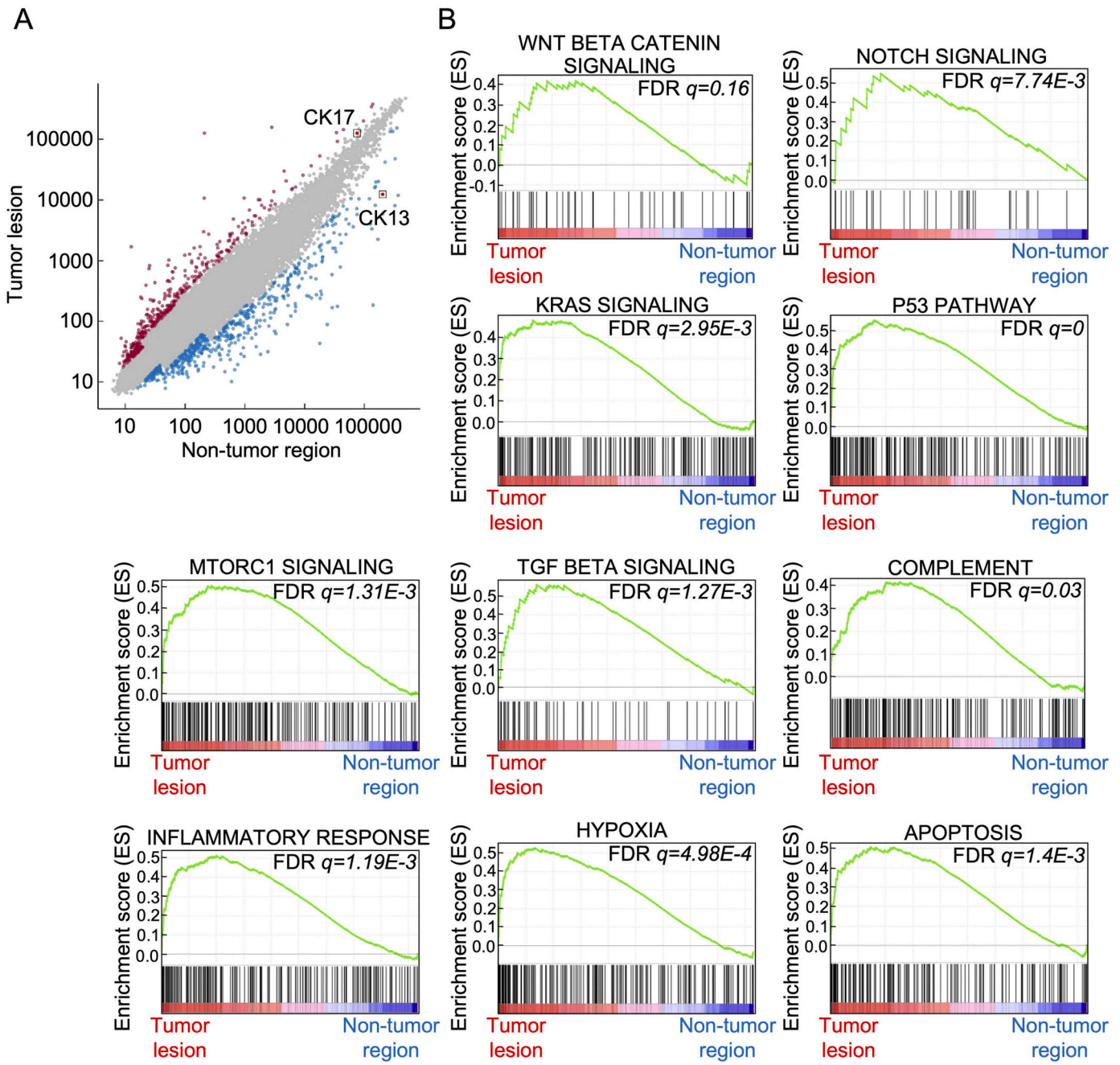

Fig. 3. The characteristics of the primary intraosseous carcinoma NOS by a DNA microarray analysis. (A) Scatterplots representing differences in gene expression amounts comparing the tumor lesion and the non-tumor region of PIOC. (B) GSEA plots show enrichment of "WNT BETA CATENIN SIGNALING", "NOTCH SIGNALING", "KRAS SIGNALING", "P53 PATHWAY", "MTORC1 SIGNALING", "TGF BETA SIGNALING", "COMPLEMENT", "INFLAMMATORY RESPONSE", "HYPOXIA", and "APOPTOSIS" related genes between tumor lesion and the non-tumor region of PIOC.

TAZ (Fig. 4C and Fig. S5C). Furthermore, consistent with a previous report [38], YAP^{5SA}, a constitutively active form of YAP [10], formed a complex with endogenous β-catenin in OSCC cells (Fig. 4D). These results suggested that the β-catenin signaling may promote YAP signaling in OSCC cells.

4. Discussion

PIOC is a diagnosis of exclusion. Therefore, histological, radiographical and clinical information is required to exclude metastasis, malignant odontogenic tumors of specific types, carcinomas of the maxillary antrum and nasal mucosa, and intraosseous salivary gland neoplasms [1]. Because the histopathological findings demonstrated a transition from odontogenic keratocyst to carcinoma, this case was diagnosed as PIOC, taking the clinical findings into account. In the present case, retrospective radiographical features showed no findings suspicious for malignancy. Considering the current findings, even in cystic cases in which malignancy is not suspected clinically, it is necessary to perform routine biopsy and pathological examination.

The immunohistochemical findings (Fig. S6), quantitative RT-PCR data and a DNA microarray analysis revealed that several oncogene-related pathways, such as Wnt/β-catenin signaling (accompanying increased expression of ARL4C), YAP signaling and Notch signaling, were activated in the present PIOC. It is generally accepted that tumor cell genomes are more hypomethylated compared to non-tumor cells [41]. Additionally, several reports have demonstrated that alterations in

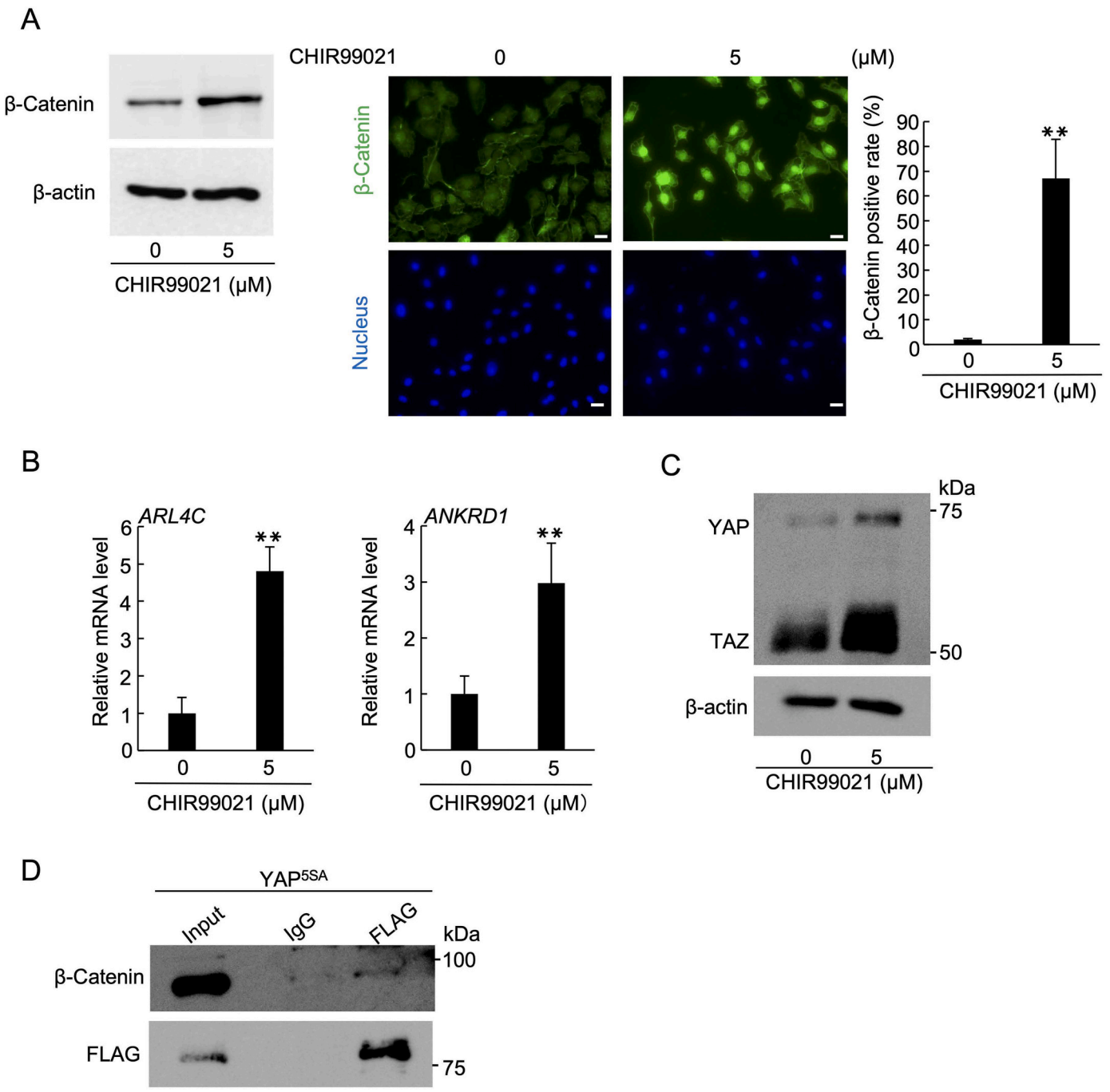

Fig. 4. Wnt/β-catenin signaling activates YAP signaling in oral squamous cell carcinoma cells. (A-C) HSC-3 cells were cultured with or without 5 μM CHIR99021 for 24 h. (A) Cell lysates were probed with anti-β-catenin and anti-β-actin antibodies (left panels). After the culture, the cells were stained with anti-β-catenin (Green) and Hoechst 33342, and then cells in which β-catenin localizes to the nucleus and Hoechst 33342-stained cells were counted, respectively (right panels and graph). (B) *ARL4C* and *ANKRD1* mRNA levels were measured by quantitative RT-PCR. Relative *ARL4C* and *ANKRD1* mRNA levels were normalized by *GAPDH* and expressed as fold-changes compared with levels in control cells. (C) Cell lysates were probed with anti-YAP/TAZ and anti-β-actin antibodies. (D) Lysates of HSC-3 cells expressing YAP^{5SA} were immunoprecipitated with control IgG or anti-FLAG antibody and the immunoprecipitates were probed with the β-catenin antibody. Scale bars, 20 μm. Results are shown as means ± s.d. of three independent experiments. $^{**}P<0.01$.

DNA methylation occur in cancer, including hypermethylation of tumor suppressor genes and hypomethylation of oncogenes [42–47]. An increase of 5mC levels and a decrease of 5hmC levels were observed in this study (see Fig. 2E), indeed suggesting a global increase in gene methylation, and thus potentially suggesting a decrease in the expression of many genes in PIOC. Consistently, the expression of 581 genes was downregulated in the tumor lesions based on DNA microarray data. On the other hand, the expression of 389 genes was upregulated (see Fig. 3A) and cell proliferation was dramatically enhanced (see Fig. 1C; upper panels) in the tumor lesions. In this study, we aimed to identify gain-of-function changes in the cellular signal transduction pathways that drive PIOC cell proliferation. Therefore, we concentrated on upregulated genes and pathways, such as Wnt/β-catenin signaling, YAP signaling and Notch signaling in DNA microarray and GSEA analyses. The data from the dot blot analysis represents global changes in DNA methylation, and it would require considerable efforts to analyze the

methylation status of individual genes. At present, we can conclude that PIOC is associated with epigenetic regulation in the methylation level, but here is no direct data to conclude how these epigenetic changes contribute to the pathogenesis of PIOC. Further studies should assess how the decreased expression of genes that are methylated in PIOC are involved in the development of PIOC.

Since it has been reported that Wnt/β-catenin signaling does not play a role in OSCC tumorigenesis [29–31], we hypothesized that Wnt/β-catenin activation observed may be related to the rarity of PIOC. Further studies should assess the association of these signal transduction pathways and/or epigenetic changes to PIOC tumorigenesis using large PIOC patient cohort.

Reportedly, Wnt/β-catenin signaling promotes YAP activity at the protein or transcriptional level [38,39]. Our present data demonstrated that Wnt/β-catenin signaling could induce YAP activity at protein level, which might be regulated through the protein association of β-catenin and YAP (see Fig. 4C and D), because CHIR99021 treatment did not affect mRNA level of *YAP* in OSCC cells (data not shown).

Odontogenic keratocyst is a developmental cyst derived from odontogenic epithelium, but is previously classified as neoplastic lesions based on their potential aggressive and infiltrative behavior [48]. This neoplastic-like potential of odontogenic keratocyst may be supported by the frequent YAP expression and its nuclear localization with high positive rate of Ki-67 staining (see Fig. S2). It is intriguing to speculate that YAP signaling is activated in odontogenic keratocyst, and the activation of Wnt/β-catenin signaling may further activate YAP signaling, which may be involved in the pathogenesis of this PIOC. In contrast, a recent report showed that Wnt/β-catenin signaling suppresses YAP signaling, which would be mildly activated, in odontogenic epithelial cells [12]. In this study, we used OSCC cells to investigate the relationship between Wnt/β-catenin signaling and YAP signaling. Since Wnt/β-catenin signaling is inactivated while YAP signaling is hyperactivated in OSCC cells [10,29–31], it is reasonable to use OSCC cells than odontogenic epithelial cells to clarify the etiology of PIOC, at least in a SCC type, derived from odontogenic keratocyst, where YAP signaling is highly activated, immunohistochemically (see Fig. 1C; middle left panel). Further studies are needed to generate an odontogenic keratocyst-derived cell line and verify our hypothesis.

In summary, we characterized a case of PIOC arising from odontogenic keratocyst by immunohistochemical analyses and proposed that further activation of YAP signaling by Wnt/β-catenin signaling may be involved in the pathogenesis of PIOC.

Funding

This work was supported by JSPS KAKENHI Grants to S.F. (2023–2025) (JP22KK0262), (2024–2027) (JP24K02615), K.H. (2021–2023) (JP21K09843), and T.K. (2023–2026) (JP23H03102), and Takeda Science Foundation, The Shinnihon Foundation of Advanced Medical Treatment Research, The Mochida Memorial Foundation for Medical and Pharmaceutical Research, TERUMO LIFE SCIENCE FOUNDATION and The Ube Industries Foundation to S.F., Takeda Science Foundation and Fukuoka Public Health Promotion Organization Cancer Research Fund and Kaibara Morikazu Medical Science Promotion Foundation to K.H., and Maritza and Reino Salonen Foundation to K.H.

CRediT authorship contribution statement

Shinsuke Fujii: Writing – original draft, Methodology, Funding acquisition, Conceptualization. **Kana Hasegawa:** Writing – original draft, Investigation, Funding acquisition. **Tamotsu Kiyoshima:** Writing – review & editing, Project administration, Funding acquisition. **Yusuke Nakako:** Investigation, Data curation. **Shintaro Kawano:** Methodology. **Kazunori Yoshiura:** Supervision. **Kristiina Heikinheimo:** Writing – review & editing, Supervision. **Kari J Kurppa:** Writing – review & editing, Supervision. **Masafumi Moriyama:** Resources. **Mizuki Sakamoto:** Resources. **Taiki Sakamoto:** Resources. **Yukiko Kami:** Supervision.

Declaration of Competing Interest

None of the authors have any relevant financial relationship(s) with a commercial interest.

Acknowledgments

The authors thank, Drs. S. Nakamura, H. Wada, TTK. Truong and T. Fujimoto and Mr H. Otoba, for valuable technical support in this research. We appreciate the technical assistance from The Joint Use Laboratories, Faculty of Dental Science, Kyushu University.

Appendix A. Supporting information

Supplementary data associated with this article can be found in the online version at doi:10.1016/j.prp.2024.155420.

References

[1] A.K. El-Nagger, J.K.C. Chan, J.R. Grandis, T. Takata. WHO classification of odontogenic and maxillofacial bone tumours. WHO classification of Head and Neck Tumours, 4th ed., IARC press, Lyon, 2017, pp. 204–209.
[2] C. Marin, M. Dave, K.D. Hunter, Malignant odontogenic tumours: a systematic review of cases reported in literature, Front Oral. Health 2 (2021) 775707, https://doi.org/10.3389/froh.2021.775707.
[3] L. Bodner, E. Manor, M. Shear, I. van der Waal, Primary intraosseous squamous cell carcinoma arising in an odontogenic cyst: a clinicopathologic analysis of 116 reported cases, J. Oral. Pathol. Med. 40 (2011) 733–738, https://doi.org/10.1111/j.1600-0714.2011.01058.x.
[4] E.F. de Morais, L.M. Carlan, H.G. de Farias Morais, J.C. Pinheiro, H.D.D. Martins, C. A.G. Barboza, R. de Almeida Freitas, Primary intraosseous squamous cell carcinoma involving the jaw bones, a systematic review and update, Head. Neck Pathol. 15 (2021) 608–616, https://doi.org/10.1007/s12105-020-01234-z.
[5] A. Keszler, M.J. Piloni, Malignant transformation in odontogenic keratocysts. Case report, Med Oral. 7 (2002) 331–335.
[6] G.J. Makowski, S. McGuff, J.E. Van Sickels, Squamous cell carcinoma in a maxillary odontogenic keratocyst, J. Oral. Maxillofac. Surg. 59 (2001) 76–80, https://doi.org/10.1053/joms.2001.19297.
[7] S. Fujii, K. Shinjo, S. Matsumoto, T. Harada, S. Nojima, S. Sato, Y. Usami, S. Toyosawa, E. Morii, Y. Kondo, A. Kikuchi, Epigenetic upregulation of ARL4C, due to DNA hypomethylation in the 3′-untranslated region, promotes tumorigenesis of lung squamous cell carcinoma, Oncotarget 7 (2016) 81571–81587, https://doi.org/10.18632/oncotarget.13147.
[8] S. Fujii, T. Ishibashi, M. Kokura, T. Fujimoto, S. Matsumoto, S. Shidara, K. J. Kurppa, J. Pape, J. Caton, P.R. Morgan, K. Heikinheimo, A. Kikuchi, E. Jimi, T. Kiyoshima, RAF1-MEK/ERK pathway-dependent ARL4C expression promotes ameloblastoma cell proliferation and osteoclast formation, J. Pathol. 256 (2022) 119–133, https://doi.org/10.1002/path.5814.
[9] D.Z.R. Alkhatib, T. Thi Kim Truong, S. Fujii, K. Hasegawa, R. Nagano, Y. Tajiri, T. Kiyoshima, Stepwise activation of p63 and the MEK/ERK pathway induces the expression of ARL4C to promote oral squamous cell carcinoma cell proliferation, Pathol. Res. Pr. 246 (2023) 154493, https://doi.org/10.1016/j.prp.2023.154493.
[10] K. Hasegawa, S. Fujii, S. Matsumoto, Y. Tajiri, A. Kikuchi, T. Kiyoshima, YAP signaling induces PIEZO1 to promote oral squamous cell carcinoma cell proliferation, J. Pathol. 253 (2021) 80–93, https://doi.org/10.1002/path.5553.
[11] K. Hasegawa, S. Fujii, K.J. Kurppa, T. Maehara, K. Oobu, S. Nakamura, T. Kiyoshima, Clear cell squamous cell carcinoma of the tongue exhibits characteristics as an undifferentiated squamous cell carcinoma, Pathol. Res. Pr. 235 (2022) 153909, https://doi.org/10.1016/j.prp.2022.153909.
[12] R. Nagano, S. Fujii, K. Hasegawa, H. Maeda, T. Kiyoshima, Wnt signaling promotes tooth germ development through YAP1-TGF-β signaling, Biochem. Biophys. Res. Commun. 630 (2022) 64–70, https://doi.org/10.1016/j.bbrc.2022.09.012.
[13] S. Fujii, K. Nagata, S. Matsumoto, K.I. Kohashi, A. Kikuchi, Y. Oda, T. Kiyoshima, N. Wada, Wnt/β-catenin signaling, which is activated in odontomas, reduces Sema3A expression to regulate odontogenic epithelial cell proliferation and tooth germ development, Sci. Rep. 9 (2019) 4257, https://doi.org/10.1038/s41598-019-39686-1.
[14] S. Fujii, S. Matsumoto, S. Nojima, E. Morii, A. Kikuchi, Arl4c expression in colorectal and lung cancers promotes tumorigenesis and may represent a novel therapeutic target, Oncogene 34 (2015) 4834–4844, https://doi.org/10.1038/onc.2014.402.
[15] S. Fujii, Y. Tajiri, K. Hasegawa, S. Matsumoto, R.U. Yoshimoto, H. Wada, S. Kishida, M.A. Kido, H. Yoshikawa, S. Ozeki, T. Kiyoshima, The TRPV4-AKT axis promotes oral squamous cell carcinoma cell proliferation via CaMKII activation, Lab Invest 100 (2020) 311–323, https://doi.org/10.1038/s41374-019-0357-z.

[16] T.T.K. Truong, S. Fujii, R. Nagano, K. Hasegawa, M. Kokura, Y. Chiba, K. Yoshizaki, S. Fukumoto, T. Kiyoshima, Arl4c is involved in tooth germ development through osteoblastic/ameloblastic differentiation, Biochem. Biophys. Res. Commun. 679 (2023) 167–174, https://doi.org/10.1016/j.bbrc.2023.09.014.
[17] Y. Mikami, S. Fujii, K.I. Kohashi, Y. Yamada, M. Moriyama, S. Kawano, S. Nakamura, Y. Oda, T. Kiyoshima, Low-grade myofibroblastic sarcoma arising in the tip of the tongue with intravascular invasion: a case report, Oncol. Lett. 16 (2018) 3889–3894, https://doi.org/10.3892/ol.2018.9115.
[18] S. Fujii, T. Fujimoto, K. Hasegawa, R. Nagano, T. Ishibashi, K.J. Kurppa, Y. Mikami, M. Kokura, Y. Tajiri, T. Kibe, H. Wada, N. Wada, S. Kishida, Y. Higuchi, T. Kiyoshima, The Semaphorin 3A-AKT axis-mediated cell proliferation in salivary gland morphogenesis and adenoid cystic carcinoma pathogenesis, Pathol. Res. Pr. 236 (2022) 153991, https://doi.org/10.1016/j.prp.2022.153991.
[19] S. Matsumoto, S. Fujii, A. Sato, S. Ibuka, Y. Kagawa, M. Ishii, A. Kikuchi, A combination of Wnt and growth factor signaling induces Arl4c expression to form epithelial tubular structures, EMBO J. 33 (2014) 702–718, https://doi.org/10.1002/embj.201386942.
[20] H. Kimura, K. Fumoto, K. Shojima, S. Nojima, Y. Osugi, H. Tomihara, H. Eguchi, Y. Shintani, H. Endo, M. Inoue, Y. Doki, M. Okumura, E. Morii, A. Kikuchi, CKAP4 is a Dickkopf1 receptor and is involved in tumor progression, J. Clin. Invest. 126 (2016) 2689–2705, https://doi.org/10.1172/JCI84658.
[21] T. Mikami, J. Cheng, S. Maruyama, T. Kobayashi, A. Funayama, M. Yamazaki, H. A. Adeola, L. Wu, S. Shingaki, C. Saito, T. Saku, Emergence of keratin 17 vs. loss of keratin 13: their reciprocal immunohistochemical profiles in oral carcinoma in situ, Oral. Oncol. 47 (2011) 497–503, https://doi.org/10.1016/j.oraloncology.2011.03.015.
[22] R. Khanom, C.T. Nguyen, K. Kayamori, X. Zhao, K. Morita, Y. Miki, K. Katsube, A. Yamaguchi, K. Sakamoto, Keratin 17 is induced in oral cancer and facilitates tumor growth, PLoS One 11 (2016) e0161163, https://doi.org/10.1371/journal.pone.0161163.
[23] Y. Mikami, S. Fujii, K. Nagata, H. Wada, K. Hasegawa, M. Abe, R.U. Yoshimoto, S. Kawano, S. Nakamura, T. Kiyoshima, GLI-mediated Keratin 17 expression promotes tumor cell growth through the anti-apoptotic function in oral squamous cell carcinomas, J. Cancer Res. Clin. Oncol. 143 (2017) 1381–1393, https://doi.org/10.1007/s00432-017-2398-2.
[24] L.J. Saucedo, B.A. Edgar, Filling out the hippo pathway, Nat. Rev. Mol. Cell Biol. 8 (2007) 613–621, https://doi.org/10.1038/nrm2221.
[25] S. Dupont, L. Morsut, M. Aragona, E. Enzo, S. Giulitti, M. Cordenonsi, F. Zanconato, J. Le Digabel, M. Forcato, S. Bicciato, N. Elvassore, S. Piccolo, Role of YAP/TAZ in mechanotransduction, Nature 474 (2011) 179–183, https://doi.org/10.1038/nature10137.
[26] Q.W. Man, Y.Q. Ma, J.Y. Liu, Y. Zhao, B. Liu, Y.F. Zhao, Expression of YAP/TAZ in keratocystic odontogenic tumors and its possible association with proliferative behavior, Biomed. Res. Int. (2017). , 4624890 10.1155/2017/4624890.
[27] R. Nusse, H. Clevers, Wnt/β-Catenin signaling, disease, and emerging therapeutic modalities, Cell 169 (2017) 985–999, https://doi.org/10.1016/j.cell.2017.05.016.
[28] S. Fujii, T. Kiyoshima, The role of Wnt, ARL4C, and Sema3A in developmental process and disease pathogenesis, Pathol. Int. 73 (2023) 217–233, https://doi.org/10.1111/pin.13325.
[29] S. Iwai, W. Katagiri, C. Kong, S. Amekawa, M. Nakazawa, Y. Yura, Mutations of the APC, beta-catenin, and axin 1 genes and cytoplasmic accumulation of beta-catenin in oral squamous cell carcinoma, J. Cancer Res. Clin. Oncol. 131 (2005) 773–782, https://doi.org/10.1007/s00432-005-0027-y.
[30] R. Tsuchiya, G. Yamamoto, Y. Nagoshi, T. Aida, T. Irie, T. Tachikawa, Expression of adenomatous polyposis coli (APC) in tumorigenesis of human oral squamous cell carcinoma, Oral. Oncol. 40 (2004) 932–940, https://doi.org/10.1016/j.oraloncology.2004.04.011.
[31] K.T. Yeh, J.G. Chang, T.H. Lin, Y.F. Wang, J.Y. Chang, M.C. Shih, C.C. Lin, Correlation between protein expression and epigenetic and mutation changes of Wnt pathway-related genes in oral cancer, Int. J. Oncol. 23 (2003) 1001–1007.
[32] E.H. Jho, T. Zhang, C. Domon, C.K. Joo, J.N. Freund, F. Costantini, Wnt/β-catenin/Tcf signaling induces the transcription of Axin2, a negative regulator of the signaling pathway, Mol. Cell Biol. 22 (2002) 1172–1183, https://doi.org/10.1128/MCB.22.4.1172-1183.2002.
[33] J.R. Miller, The Wnts, Reviews3001, Genome Biol. 3 (2002), https://doi.org/10.1186/gb-2001-3-1-reviews3001.
[34] C.X. Song, C. He, Balance of DNA methylation and demethylation in cancer development, Genome Biol. 13 (2012) 173, https://doi.org/10.1186/gb-2012-13-10-2012.
[35] H. Meng, Y. Cao, J. Qin, X. Song, Q. Zhang, Y. Shi, L. Cao, DNA methylation, its mediators and genome integrity, Int. J. Biol. Sci. 11 (2015) 604–617, https://doi.org/10.7150/ijbs.11218.10.7150/ijbs.11218.
[36] N. Sethi, Y. Kang, Notch signalling in cancer progression and bone metastasis, Br. J. Cancer 105 (2011) 1805–1810, https://doi.org/10.1038/bjc.2011.497.
[37] K. Sakamoto, Notch signaling in oral squamous neoplasia, Pathol. Int 66 (2016) 609–617, https://doi.org/10.1111/pin.12461.
[38] T. Liu, L. Zhou, K. Yang, K. Iwasawa, A.L. Kadekaro, T. Takebe, T. Andl, Y. Zhang, The β-catenin/YAP signaling axis is a key regulator of melanoma-associated fibroblasts, Signal Transduct. Target Ther. 4 (2019) 63, https://doi.org/10.1038/s41392-019-0100-7.
[39] W.M. Konsavage Jr., S.L. Kyler, S.A. Rennoll, G. Jin, G.S. Yochum, Wnt/β-catenin signaling regulates Yes-associated protein (YAP) gene expression in colorectal carcinoma cells, J. Biol. Chem. 287 (2012) 11730–11739, https://doi.org/10.1074/jbc.M111.327767.
[40] D.B. Ring, K.W. Johnson, E.J. Henriksen, J.M. Nuss, D. Goff, T.R. Kinnick, S.T. Ma, J.W. Reeder, I. Samuels, T. Slabiak, A.S. Wagman, M.E. Hammond, S.D. Harrison, Selective glycogen synthase kinase 3 inhibitors potentiate insulin activation of glucose transport and utilization in vitro and in vivo, Diabetes 52 (2003) 588–595, https://doi.org/10.2337/diabetes.52.3.588.
[41] R. Brown, G. Strathdee, Epigenomics and epigenetic therapy of cancer, Trends Mol. Med. 8 (2002) S43–S48, https://doi.org/10.1016/s1471-4914(02)02314-6.
[42] S.B. Baylin, M. Esteller, M.R. Rountree, K.E. Bachman, K. Schuebel, J.G. Herman, Aberrant patterns of DNA methylation, chromatin formation and gene expression in cancer, Hum. Mol. Genet. 10 (2001) 687–692, https://doi.org/10.1093/hmg/10.7.687.
[43] H. Kim, Y.M. Kwon, J.S. Kim, J. Han, Y.M. Shim, J. Park, D.H. Kim, Elevated mRNA levels of DNA methyltransferase-1 as an independent prognostic factor in primary nonsmall cell lung cancer, Cancer 107 (2006) 1042–1049, https://doi.org/10.1002/cncr.22087.
[44] M. Fabbri, R. Garzon, A. Cimmino, Z. Liu, N. Zanesi, E. Callegari, S. Liu, H. Alder, S. Costinean, C. Fernandez-Cymering, S. Volinia, G. Guler, C.D. Morrison, K. K. Chan, G. Marcucci, G.A. Calin, K. Huebner, C.M. Croce, MicroRNA-29 family reverts aberrant methylation in lung cancer by targeting DNA methyltransferases 3A and 3B, Proc. Natl. Acad. Sci. USA 104 (2007) 15805–15810, https://doi.org/10.1073/pnas.0707628104.
[45] R.K. Lin, H.S. Hsu, J.W. Chang, C.Y. Chen, J.T. Chen, Y.C. Wang, Alteration of DNA methyltransferases contributes to 5′CpG methylation and poor prognosis in lung cancer, Lung Cancer 55 (2007) 205–213, https://doi.org/10.1016/j.lungcan.2006.10.022.
[46] R.K. Lin, C.Y. Wu, J.W. Chang, L.J. Juan, H.S. Hsu, C.Y. Chen, Y.Y. Lu, Y.A. Tang, Y.C. Yang, P.C. Yang, Y.C. Wang, Dysregulation of p53/Sp1 control leads to DNA methyltransferase-1 overexpression in lung cancer, Cancer Res. 70 (2010) 5807–5817, https://doi.org/10.1158/0008-5472.CAN-09-4161.
[47] S.H. Lin, J. Wang, P. Saintigny, C.C. Wu, U. Giri, J. Zhang, T. Menju, L. Diao, L. Byers, J.N. Weinstein, K.R. Coombes, L. Girard, R. Komaki, I.I. Wistuba, H. Date, J.D. Minna, J.V. Heymach, Genes suppressed by DNA methylation in non-small cell lung cancer reveal the epigenetics of epithelial-mesenchymal transition, BMC Genom. 15 (2014) 1079, https://doi.org/10.1186/1471-2164-15-1079.
[48] Leon Barnes, John W. Eveson, Peter Reichart, David Sidransky, Odontogenic tumours. WHO classification of Head and Neck Tumours, IARC press, Lyon, 2005, pp. 306–307.